PREPARATION AND PROPERTIES OF Nb JOSEPHSON JUNCTIONS WITH THIN Al LAYERS

by

M. Gurvitch, M. A. Washington, H. A. Huggins, and J. M. Rowell
Bell Laboratories
600 Mountain Avenue
Murray Hill, NJ 07974

Abstract

Josephson tunnel junctions of the types Nb/Al-oxide-Nb and Nb/Al-oxide-Al/Nb, where Al represents thin ($\sim$50Å) films of Al, were prepared by D.C. magnetron sputtering. The tunnel barrier was formed by in-situ thermal oxidation. Individual junctions were defined using photolithography coupled with the plasma etching technique. Junctions with critical current density up to 1300 A/cm^2 and $V_m = i_c R(2mV)$ between 15mV and 47mV at 4.2K were obtained.

1. Introduction

The well-known desirable properties of Nb as a material for Josephson tunnel junctions include a T_c of 9.3K and mechanical ruggedness. In principle Nb with an appropriately grown native oxide barrier can be used to form hard tunnel junctions.[1] However, then one has to put up with the disadvantage of having the high dielectric constant ε of Nb oxide and, more importantly, with the well-known difficulty of producing high quality (i.e., high Vm) all-Nb junctions. This work centers on resolving these problems by employing thin layers of Al near the barrier. It was shown previously[2] that a system consisting of a Nb film covered with a thin layer of Al possesses very fortunate properties in that even a thin layer of Al appears to "wet", i.e., uniformly cover the surface of Nb, hence preventing the formation of the native oxides of Nb.[3] The tunnel barrier can be formed by a simple thermal oxidation of the Al overlayer. The stable, low ε Al oxide allows then a deposition of a hard counterelectrode.[4] We show in this work that tunnel junctions formed in this way have unprecedented high quality as far as all-Nb structures are concerned, and can even be favorably compared in quality to typical junctions with soft counterelectrodes.

2. Formation of the Tunneling Structure

The basic Nb/Al-oxide-(Al)/Nb (the second Al layer is optional) sandwich structure was formed in an oil diffusion pumped vacuum system equipped with three D.C. magnetron sputtering guns, a large liquid nitrogen Meissner trap and a rotating substrate table.[5] Sputtering was done in 15 mtorr of Ar (99.9995% pure), with the main valve of the vacuum system being partially closed. The background pressure in this configuration is typically $\sim$2.10^{-7} torr. Together with impurities in Ar, this amounts to about 3.10^{-7} torr of unwanted gases in the chamber: presumably hydrogen, water vapor, nitrogen and oxygen. Assuming a sticking coefficient of 1.0 for these gases, this corresponds to 0.1 - 0.2Å/sec absorption rate on the surface of a substrate, i.e., about one monolayer in 10 sec. The deposition rate of Nb is $\sim$13Å/sec. Hence, in principle, impurities may amount to $\sim$1 at. % of the deposited Nb film. However, the T_c's o these films do not differ from the bulk value of 9.3 $\pm$ 0.1K, indicating that at least the amount of oxygen in the film is much smaller than 1% (oxygen is known to reduce the T_c of Nb by $\sim$1K per 1 at. % [6]).

All depositions are done without any intentional heating of the substrate. The temperature of a small unsupported thermocouple placed near the substrate rises to $\sim$150°C in 3.5 min. The substrate (oxidized silicon), which rests on a massive stainless steel holder, may have a somewhat lower temperature. Indeed, Nb was deposited on substrates covered with photoresist patterns: subsequent lift-off was successfully done by soaking the sample in acetone, which indicates that photoresist was not warmed up above $\sim$120°C. Nb films are microcrystalline, with grains being oriented with (110) direction normal to the film. The grain size is of the order of 100Å as evidenced by TEM. Detailed X-ray measurements of D. B. McWhan put the lower limit for the grain size at $\sim$80Å. It is instructive to relate these numbers with the resistance ratio (r.r.) of our films, which is 4-5. Let us estimate the electronic mean free path ℓ in Nb at room temperature: $\ell = \langle v_F^2 \rangle^{1/2} \cdot \tau$, where $\langle v_F^2 \rangle^{1/2} = 6.1 \cdot 10^7$ cm/sec is the average Fermi velocity of Nb calculated by Chakraborty et. al.[7] and the relaxation time τ can be estimated from the relation[8] $\hbar/\tau = 2\pi K_B T\lambda$ ($T > \theta_D$), where $\lambda = 1.0 \pm 0.1$ is the electron-phonon coupling constant of Nb.[9] Substituting the numbers we obtain $\ell(300K) \simeq 25$Å. Taking r.r. = 4.5 we find $\ell(10K) = 4.5 \times 25 = 112$Å. This value is in remarkable agreement with independent estimates of the grain size. We conclude that the mean free path in our films is limited by grain boundary scattering. This is further confirmed by the observation that Nb films prepared at elevated substrate temperatures are known to have larger grains and higher r.r. The apparent absence of impurity scattering together with observed bulk T_c's suggests high purity of our Nb films.

Multilayered tunneling structures were prepared by depositing Nb base electrodes $\sim$2500Å thick, starting the Al gun, and moving the substrate table at a specified speed, so that the substrate passes under the Al gun. The time between the end of Nb deposition and the beginning of Al deposition is typically 30-45 sec. As was said, the pressure of unwanted gases in the system is $\sim$3 · 10^{-7} torr. In principle, in this vacuum, about 3 monolayers of impurities can be deposited on a sample surface in 30 sec. In reality the contamination, if present at all, is very much smaller, as evidenced by XPS (see J. R. Kwo et. al. in this volume). This fact is in agreement with the apparent cleanliness of Nb films and must reflect the low partial pressure of oxygen.

The nominal thickness of the Al overlayer (typically 40-50Å) was determined from the independently measured deposition rate of Al, speed of table rotation and the size of the opening in the shield. (It is assumed that the sticking coefficient of Al on Nb is the same as that of Al on Al and independent on the Al overlayer thickness.) The actual thickness of the Al overlayer on Nb can be considerably smaller than the nominal one due to the grain boundary diffusion of Al into the bulk of Nb.[3] The intergrain Al does not seem to influence superconductivity of Nb; at least we do not see any depression of the superconducting gap of Nb for nominal Al overlayer thicknesses up to $\sim$30Å.* Hence grain boundary diffusion of Al provides a convenient mechanism for self-regulation of the Al overlayer thick-

---

* We measure $\Delta_{Nb}(o) = 1.57$mV on samples with Pb-Bi counterelectrodes: this is the bulk gap of Nb (see also J. R. Kwo et. al. in this volume).

ness. This may ease the requirements for Al thickness control and will be helpful in reproducing the same critical current of Josephson junctions.

After the deposition of the Al overlayer, it was oxidized in-situ in 1 torr of pure oxygen for 90 minutes. Then the system was pumped for 45 minutes and the (Al)/Nb counterelectrode was deposited in the same manner as the base electrode, only in reverse order. This completes the formation of the tunneling structure which, at this point, covers the whole substrate.

3. Sample Processing

Individual junctions were defined by placing photoresist pads over the desired areas (Figure 1a) and subjecting the exposed surface of the sample to r.f. plasma etching in 1 torr of 90% CF_4, 10% O_2 gas mixture (Figure 1b). The rate of Nb etching was 200-400Å/min at the r.f. power level of 25 watts. Etching did not proceed beyond the Al oxide barrier which, despite being as thin as 10-15 Å (see below), proved to be a very effective stop for the etching process. The next step consists of providing an insulating layer by using liquid anodization of the exposed area to 20-40v, thus creating ~400-900 Å of the anodic oxide of Nb (Figure 1c). Then the photoresist pad is removed, and the top surface of a counterelectrod is cleaned by ion milling or r.f. sputter etching. (Figure 1c). A strip of either Nb or Pb-Bi is deposited over the cleaned surface in order to make contact to the junction (Figure 1d). The whole process is similar to the Selective Niobium Anodization Process (SNAP) developed by Kroger et. al.; we call it SNEP (E for Etching). We are working on a completely dry process in which an insulator is deposited separately. Somewhat similar technologies based on the in-situ prepared tunnel structure with subsequent top electrode patterning were recently described in the literature[11] and mentioned in talks[12] by others. The distinctive feature of our process is the use of plasma or reactive ion etching (i.e., a dry, chemically active process) which allows the utilization of a very convenient Al oxide barrier stop.
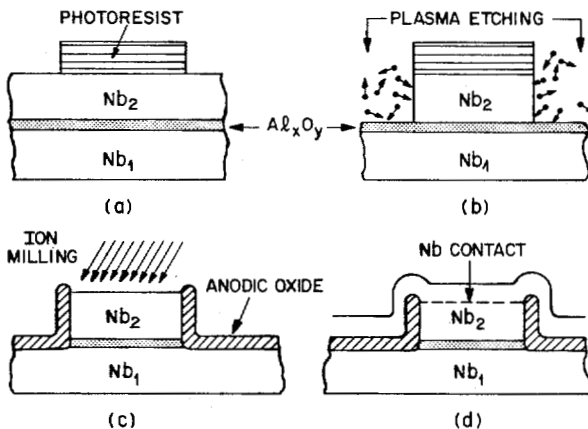

Fig. 1. Processing steps in SNEP.

4. Junction Characteristics

(i) **Critical current density**. Junctions of the type Nb/Al-oxide-Al/Nb with the nominal Al layer thickness of 50±5Å have j_c = 550±100A/cm² when oxidized in 1 torr of O_2 for 90 minutes. The reproducibility of this value in different runs was rather good, provided samples with decent I-V characteristics were obtained. Unfortunately,

the yield of SNEP samples was not sufficiently high to investigate the dependence of j_c on oxidation time and on the thickness of the Al layer in more detail. For the same oxidation conditions, samples of the type Nb/Al-oxide-Nb have j_c which is ~2-3 times higher: a clear indication that the top Al layer protects the oxide from reacting with the Nb counterelectrode.

(ii) **I-V curves, Vm, and Interference Pattern**. Representative I-V curves taken at 4.2K for both kinds of junctions are shown on Figure 2a,b. The figures of merit V_m = $i_c R(2mV)$ of these junctions are 15mV and 25mV, respectively. I-V characteristics (a recorder trace; critical current is not shown) of another sample of the type Nb/Al-oxide-Al/Nb, taken at 4.2K (solid line) and 2.0K (dashed line) are shown on Figure 2c. In this case V_m values are 35mV at 4.2K and 262mV at 2.0K. Our best junctions have V_m = 47mV at 4.2K. The conditions which lead to the highest V_m values are being investigated. The interference pattern taken on a junction from Figure 2b is shown on Figure 3. It is practically indistinguishable from an ideal one, indicating a high degree of Josephson current uniformity over the junction area.

(iii) $\Delta_1(0) + \Delta_2(0)$. The gap of bulk Nb at T=0 is $\Delta(0) = 1.56\pm0.01mV$.[13] Hence the maximum possible value of $\Delta_1(0) + \Delta_2(0)$ in our junctions is 3.12±0.02mV. In our best junctions (those which have V_m = 47mV) we measure $\Delta_1(0) + \Delta_2(0) = 3.0mV$. More typical values are 2.95±0.04mV for Nb/Al-oxide-Nb junctions and 2.74±0.05mV for Nb/Al-oxide-Al/Nb junctions. There are indications that the gap of a base electrode corresponds to the full gap of Nb, while that of a counterelectrode is somewhat reduced. This may be a result of the counterelectrode interactions with the oxide barrier (especially in Nb/Al-oxide-Nb junctions), or simply a reflection of the fact that in the base electrode the near-barrier layer of Nb is grown last, while in the counterelectrode the near-barrier layer is grown first. Hence there is a possibility of greater disorder in the near-barrier layer of the counterelectrode.

(iv) $i_c R_n$. The theoretical weak-coupling value of the product $i_c R_n$ (where R_n is the normal state resistance of a junction), for the case of equal gaps $\Delta_1 = \Delta_2 = \Delta$, is given by the Ambegaokar-Baratoff[13] expression

$$i_c R_n = \frac{\pi\Delta(T)}{2e} \tanh \frac{\Delta(T)}{2K_B T}$$

No analytical formula exists for the case $\Delta_1 \neq \Delta_2$; however, if $\Delta_1 \simeq \Delta_2$ the above expression will not introduce serious errors. Using the average value of

$$\frac{\Delta_1(4.2K) + \Delta_2(4.2K)}{2} = 1.4mV$$

we obtain $i_c R_n \simeq 2.0mV$. We observe values of $i_c R_n$ between 1.5mV and 1.85mV, the higher values corresponding to junctions with less Al, in particular to Nb/Al-oxide-Nb junctions. The $i_c R_n$ values in the range 1.7-1.85mV can be accounted for by the depression of i_c due to relatively strong coupling[15] of Nb ($\lambda = 1.0$). Smaller values of $i_c R_n$ must be associated with the proximity tunneling[16] in the presence of Al.

(v) t/ε and oxide thickness t. In digital circuit applications of Josephson junctions the reduced oxide thickness t/ε is an important parameter which determines the switching speed of a device: larger t/ε implies faster switching. The native oxide of Nb has ε ~30 and, in junctions with j_c ~ 500 A/cm², t/ε ~ (0.6-1.0)Å[17], which implies t = (18-30)Å for Nb oxide. We

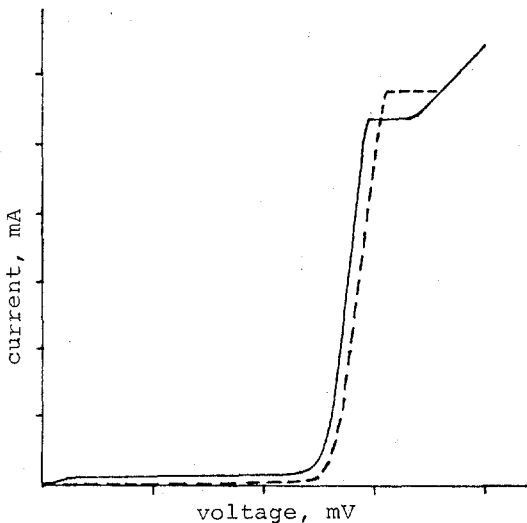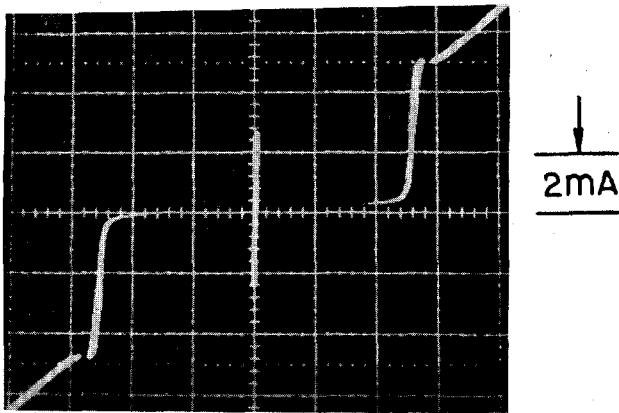**(a)**

1mA

1mV

(b)

2mA

current, mA
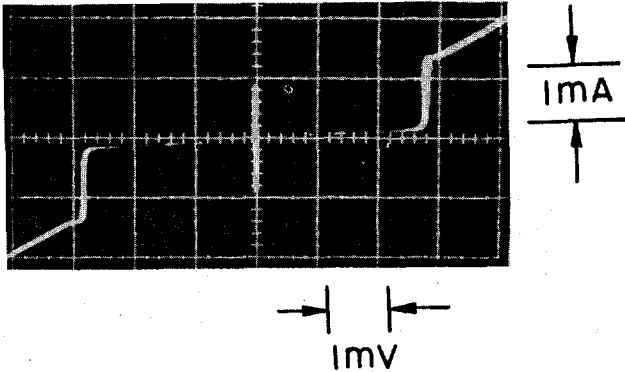
voltage, mV

Fig. 2. Current-voltage characteristics of three junctions oxidized in-situ in 1 torr of O_2 for 90 min. T = 4.2K, unless specified otherwise.

(a) Nb/Al-oxide-Nb junction, size $8 \times 8\mu m^2$, $j_c = 1300$ A/cm^2, $V_m = 15$mV.

(b) Nb/Al-oxide-Al/Nb junction, size $20 \times 20\mu m^2$, $j_c = 600$ A/cm^2, $V_m = 25$mV.

(c) Nb/Al-oxide-Al/Nb junction, size $20 \times 20\mu m^2$, $j_c = 645$ A/cm^2 (not shown). Solid curve: T = 4.2K, $V_m = 35$mV; dashed curve: T = 2.0K, $V_m = i_c \cdot R(2mV) = 262$mV and $V_m = i_c \cdot R(1.7mV) = 383$mV.

measured t/ε using Fiske resonances and found $t/\varepsilon = (1.6 \pm 0.5)$Å. The dielectric constant of Al_2O_3 is ~ 8,[18] i.e., ~ 3.5 times lower than ε of Nb_2O_5. Since our t/ε is not 3.5 times higher than that of Nb oxide, the oxide thickness in our case must be smaller. Indeed, as was found previously,[2] barriers grown on the oxidized Al overlayer are higher and thinner than those obtained on Nb. From $t/\varepsilon = 1.6$ and $\varepsilon = 8$ we find t = 12.8Å. This number is in fine agreement with an estimate of a barrier width obtained in Ref. 2 via high bias conductance measurements: $t = 13.5 \pm 1$Å.

5. Series arrays. Uniformity.

In order to check the uniformity of a critical current on a chip and to study the cycling stability of our junctions, several strings of junctions connected in series were prepared by SNEP. Each string occupied an area of 1.8 mm × 0.8 mm and consisted of 50 10 × 10μm^2 junctions. The tunneling structure was Nb/Al (46Å)-oxide (1 torr, O_2, 90 min)-Nb, with critical current densities ~ 1200 A/cm^2. An I-V curve for one of the strings is shown on Fig. 4. In this case the uniformity of the
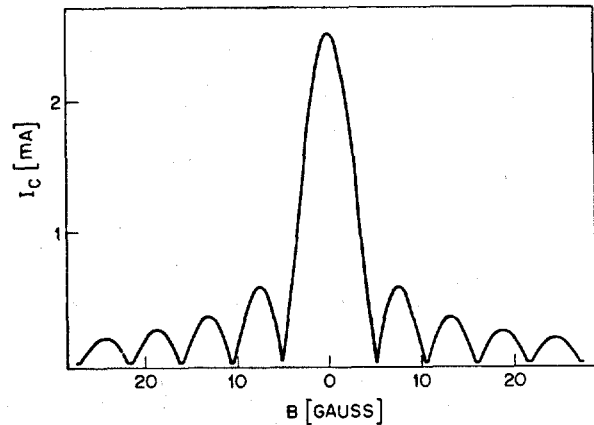

Fig. 3. Critical current vs. magnetic field for the tunnel junction whose I-V curve is shown in Fig. 2(b).

critical current along the string is $\pm 5\%$; a value typical of all good strings that were measured. Cycling results obtained on these strings by J. V. Gates are extremely encouraging. They will be reported elsewhere.
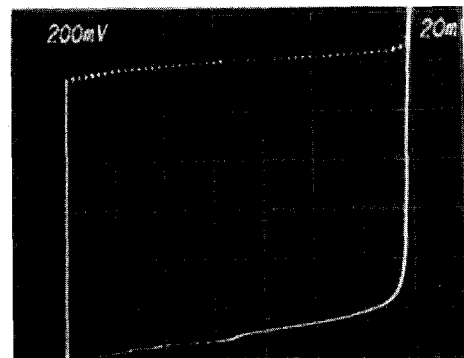

Fig. 4. An I-V curve taken on a string of 50 junctions connected in series. X axis: voltage, 20 mV per division; Y axis: current, 0.2mA per division.

6. Conclusions

The use of Al overlayers in the formation of Nb tunnel junctions is shown to bring considerable benefits. Virtually all junction parameters are improved compared to the best all-Nb junctions with native Nb oxide. In particular, the quality of the I-V curve as characterized by the figure of merit V_m is improved dramatically. These improvements are based on the fortunate combination of factors found in the Nb-Al system. Futhermore, Al oxide, known to produce some of the best tunnel barriers, appears to be very useful in processing as well (SNEP).

Preliminary results on the uniformity and stability of junctions with Al layers are encouraging.

However, the questions of confidence in consistently obtaining good samples still remain open. This problem is presently being addressed.

Acknowledgements

References

1. R. F. Broom, S. I. Raider, A. Gosenbrug, R. E. Drake and W. Walter, IEEE Trans. on Electron Devices, Vol. ED-27, No. 10, 1998 (1980).

2. J. M. Rowell, M. Gurvitch and J. Geerk, Phys. Rev. B, 24, 2278 (1981).

3. J. Kwo, G. K. Wertheim, M. Gurvitch and D. N. E. Buchanan, Appl. Phys. Lett. 40(8), 675 (1982).

4. M. Gurvitch, J. M. Rowell, H. A. Huggins, M. A. Washington and T. A. Fulton, IEDM-81, p. 115 (1981).

5. H. A. Huggins, M. Gurvitch, accepted for publication in the J. of Vac. Sci. and Tech.

6. W. DeSorbo, Phys. Rev. 132, 107 (1963).

7. B. Chakraborty, W. E. Pickett, and P. B. Allen, Phys. Rev. B, 14, 3227 (1976).

8. P. B. Allen, Phys. Rev. B 3, 305 (1971).

9. E. L. Wolf, J. Zasadzinski, J. W. Osmun, and G. B. Arnold, J. of Low Temp. Phys. 40, 19 (1980); also, J. Geerk, M. Gurvitch, D. B. McWhan, and J. M. Rowell, Physica 109 & 110B, 1775 (1982).

10. H. Kroger, L. N. Smith, and D. W. Jillie, Appl. Phys. Lett. 39(3), 280 (1981).

11. G. K. Hohenwarter and J. E. Nordman, Appl. Phys. Lett. 40(5), 436 (1982).

12. E. J. Cukauskas, APS Bulletin, 27, No. 3, 205, DE3 (1982).

13. J. Bostock, K. H. Lo, W. N. Cheung, V. Diadiuk, and M. L. A. MacVicar, in Superconductivity in d- and f-band Metals, Second Rochester Conf., D. H. Douglas (Ed.), New York: Plenum Press 1976; also in J. R. Kwo, G. K. Wertheim, M. Gurvitch, and D. N. E. Buchanan, this volume.

14. V. Ambegaokar and A. Baratoff, Phys. Rev. Lett. 11, 104 (1963).

15. T. A. Fulton and D. E. McCumber, Phys. Rev. 175, 585 (1968); D. M. Ginsberg, R. E. Harris and R. C. Dynes, Phys. Rev. B 14, 990 (1976).

16. W. J. Gallagher, Proceedings of the LT-16, Physica 108B, 825 (1981).

17. R. F. Broom, J. of Appl. Phys. 47, 5432 (1976); J. H. Magerlein, IEEE Trans. Mag., MAG-17, 286 (1981).

18. E. Schabowska, J. Szczeklik, Thin Solid Films, 75, 177 (1981).